Wide Band Raised Printed Monopole for Automotive 5G Wireless Communications

AHMAD M. YACOUB[ID], MOHAMED O. KHALIFA[ID], AND DANIEL N. ALOI (Senior Member, IEEE)

Department of Electrical and Computer Engineering, Oakland University, Rochester, MI 48309, USA

CORRESPONDING AUTHOR: A. M. YACOUB (e-mail: ahmadyacoub@oakland.edu)

ABSTRACT This paper introduces a compact Multiple input Multiple output (MIMO) antenna system for vehicular application in the sub-6GHz 5G systems that operates in the middle and high frequency bands from 1.71GHz to 5GHz. The proposed design consists of two symmetrical raised printed monopoles on Flame Retardant 4 (FR4) dielectric material with Partial Ground Plane (PGP) structure to improve bandwidth impedance and achieve higher isolation across the operating frequency range. The design is an excellent candidate to be implement in a shark-fin housing due to its low-profile characteristics and good electrical performance. The antennas are simulated using HFSS software and then prototypes are made and measured on a one-meter rolled-edge ground plane in an anechoic chamber. The electrical performance results of the proposed design and its MIMO characteristics are discussed and plotted in terms of Voltage Standing Wave Ratio (VSWR), passive isolation, radiation patterns, radiation efficiency, linear average gain (LAG), Diversity Gain (DG), and Envelope Correlation Coefficient (ECC).

INDEX TERMS MIMO, 5G, ECC, automotive shark-fin antennas, wireless vehicular communications.

I. INTRODUCTION

THE RAPID increase in development for advanced wireless communication systems has led to high demand for these systems to be deployed in the automotive field. The vehicle structure has transformed to a smart device consisting of many sensors and wireless technologies to support autonomous driving standards. 5G and Vehicle-to-everything (V2X) communications has evolutionized wireless technologies compared to the previous systems such as Bluetooth, WLAN, 2G (GSM), 3G (UMTS) and LTE. 5G and V2X are upcoming standards for vehicle communication with surrounding environment including Vehicle-to-Infrastructure (V2I), Vehicle-to-Vehicle (V2V), and Vehicle-to-Pedestrian (V2P). These communications require very low latency, high speed data rate, higher reliability, efficient power usage, and the ability to handle high number of nodes which is essential in self-driving technology, improving traffic safety, and connecting the vehicle to different nodes in an Internet of Things (IoT) network [1], [2].

The 5G network consists of two frequency bands: sub-6GHz band from 617MHz-5GHz and milli meter Waves (mmWaves) from 28 GHz up to 40GHz [3]–[4].

The wide increase in bandwidth with advanced modulations schemes compared to legacy wireless communications has helped 5G network to achieve data rates up to 10Gbps, maximum latency of 1 milli second (msec), high capacity of user nodes, and up to hundred times better power usage efficiency [5]–[6].

To achieve the requirements for 5G and V2X autonomous communications, multiple input multiple output (MIMO) antenna system should be implemented. MIMO systems have many antenna elements placed at both receiver and transmitter that operate at the same frequency range which will increase the number of channels across the radio frequency (RF) link, and hence significantly improving the total data rate and throughput in the network without increasing the transmit power or enlarging the frequency band [7]–[8]. The RF performance of the MIMO system is very dependable on the efficient design of the antenna elements. The antennas should have a good radiation efficiencies and high isolation or very low correlation between them which will result in very reliable and low latency system even in a highly scattering electromagnetic environment [9]. The Envelope Correlation Coefficient (ECC) is an important

parameter that is used to measure the correlation between the antenna elements. A low value of ECC (ideally zero) shows a high isolation (low correlation) between the antennas that results in independent RF channels in the system which is needed to achieve the required MIMO performance [10].

The MIMO antenna design in the automotive field has many limitations that affects its performance. Physical dimensions, size limitations, and interference (coupling) between different antennas are challenging issues specially if the antennas are placed in one housing. These challenges make it hard to meet the standards of MIMO performance in terms of radiation efficiency, isolation, and diversity specially when multiple applications are implemented in one single housing such as: AM/FM, Digital Audio Broadcast (DAB), cellular 5G, Satellite Digital Audio Radio System (SDARS), Dedicated Short Range Communications (DSRC), Global Navigation Satellite system (GNSS) [11].

In this paper, a novel wide band raised printed monopole with defected ground has been developed for vehicular applications that has unique shape and physical dimensions which makes it suitable for placement inside a shark-fin module on the car's roof. The proposed design can cover wide frequency bands from 1.71GHz-5GHz with reasonably small dimensions because of its unique shape in addition to using slots, partial ground plane (PGP) structures. A 2x2 MIMO antenna system is also analyzed to achieve the high-performance requirements for 5G communications. The proposed MIMO system was able to achieve good performance and isolation between elements by using ground plane structure on the back side of the monopole that improves passive isolation without increasing spatial distance between the elements specially at lower frequency bands. Compared to our previous work in [1], [2], [7], and [8], the proposed design in this paper provides a smaller footprint by using Flame Retardant (FR4) as dielectric material to reduce the overall occupied volume of the radiating element while maintaining a very good RF performance. In [12], and [13], the authors presented a printed antenna elements with a bit bigger dimension, however, the designs operate from (3GHz to 6GHz) and doesn't cover the lower frequency bands starting from 1.71GHz. In [14], and [15], 2x2 MIMO antenna systems are presented for automotive application, however, the high frequency bands don't go up to 5GHz and the physical dimensions of the high band section of the element are bigger than the proposed design in this paper. The work in [20], and [21] describes the MIMO performance for 5G sub-6GHz for smart phone applications covering the bands from 3.4GHz to 6GHz, and compared to proposed design, the elements don't cover lower frequency band starting from 1.71GHz that would require bigger height, volume, and increased spatial distance for better isolation between elements. Table 3 summarizes the comparison between existing work in literature and work presented in this paper.

The antenna element and the MIMO system proposed in this work are modeled using HFSS simulation software and then a proper prototype was made and measured on 1-meter
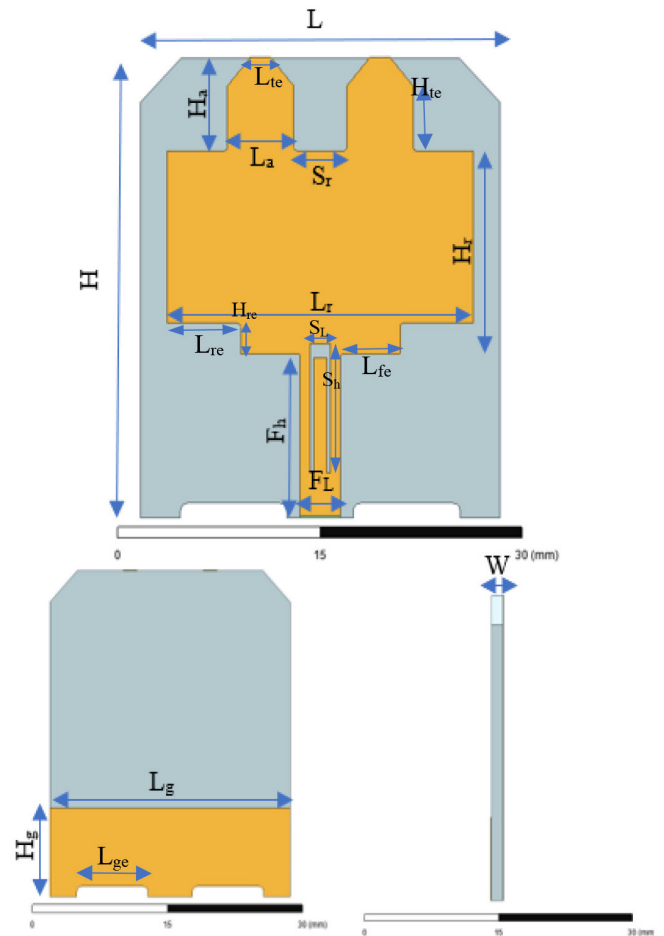

FIGURE 1. Simulated antenna with front, back and side views with its geometrical parameters.

ground plane in an anechoic chamber to present real time data for various RF properties including Voltage Standing Wave Ratio (VSWR), passive isolation, radiation patterns, electric field intensity, current distribution, antenna radiation efficiency, linear average gain (LAG), ECC, and DG.

This paper consists of the following sections: Section II discusses the proposed element design, geometrical parameters, simulation and measurement setups, and RF performance of the individual element. Section III presents the proposed MIMO antenna system, and its MIMO characteristics and performance with a table of comparison to existing work in literature.

II. PROPOSED ELEMENT DESIGN AND PERFORMANCE

The design consists of raised monopole printed on FR4 material with dielectric constant (ϵ_r) of 4.4, permeability of 1, loss tangent of 0.025, and high mechanical strength and insulating characteristics with low cost which makes it an excellent candidate for a substrate material. Fig. 1 and Table1 shows the antenna layout and its optimized geometrical parameters with total dimensions of 30mm (height) x 27mm (length) x 1mm (width or substrate thickness).

TABLE 1. Values of the optimized geometrical parameters of the proposed antenna.

Parameter	Value (mm)	Parameter	Value (mm)
H	30	Lg	27
L	27	Hg	8
W	1	Sr	4
Ha	6.25	Lr	23
La	5.25	Hr	12.75
F_h	11	F_L	3
L_{ge}	7.8	L_{te}	1.5
L_{re}	5.25	L_{fe}	4.25
S_L	1.5	S_h	9
H_{te}	4.2	H_{re}	1.85

TABLE 2. Design goals and performance specifications.

Parameter	Value
Polarization	Vertical Linear Polarization (VLP)
VSWR	3.3:1 VSWR at 5G frequency bands
Efficiency	60%
LAG	-4dBi across theta (75-87) at 5G

(a) front view (b) back view

FIGURE 2. Fabricated antenna prototype with front and back views.
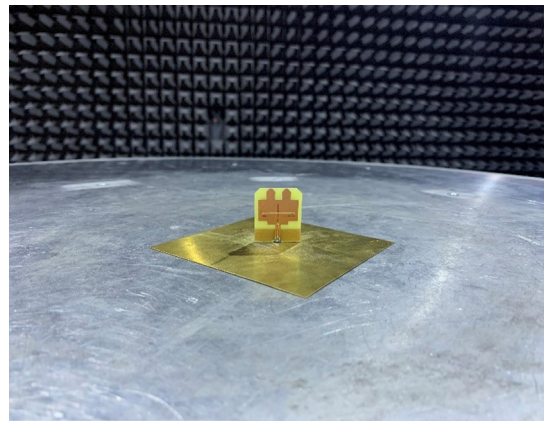

FIGURE 3. Antenna Setup on ground plane.

The monopole structure consists of feeding line and wide rectangular shape with two branches. The feed line has a height of 11mm (F_h) and a width of 3mm (F_L) that feeds the rectangular shape with RF signal. A reversed U-shape slot is constructed along the feed line to increase the traveling path of RF current which supports higher wavelengths and hence helps tune the antenna towards lower frequency bands. The wide rectangular shape is excited by the feed line, its height and length allow the antenna to operate across the whole frequency range from 1.71GHz to 5GHz in addition to two branches connected to the structure that will increase the total height of the element to make the element operate at lower frequency bands. As a guideline for the antenna design, the feed line, and the rectangular shape with two branches should be loaded at $\frac{\lambda_c}{4}$ distance from the ground plane where λ_c is the center frequency of the operating frequency range ($f_c = 2.5$GHz) to provide good impedance matching and radiation pattern values. The length of the wide rectangular shape increases the total volume of the antenna and hence allows it to cover a wide frequency range. The FR4 material and the reversed U-shape slot will load the antenna element and further increase the current path which enables the design to operate at lower frequencies.

The partial ground plane shape on the back side has a height of 8mm (Hg) and a length of 27mm (Lg). This structure has significant effect on improving the VSWR of the antenna and provides a better isolation between the elements in the MIMO system as presented in the next section. The height and length of the PGP were optimized to improve the impedance bandwidth across the operating bands and to reduce the mutual coupling between the elements. Fig. 2 shows the fabricated antenna prototype with front and back views.

Table 2 presents the design goals and requirements for antenna performance for vehicular applications in terms of polarization, VSWR, radiation efficiency, and LAG. VSWR requirement is better than 3.3:1 for 5G frequency bands with LAG higher than −4dBi at theta from (75-87 degrees) as specified by many automotive Original Equipment manufacturers (OEMs) [1]–[2].
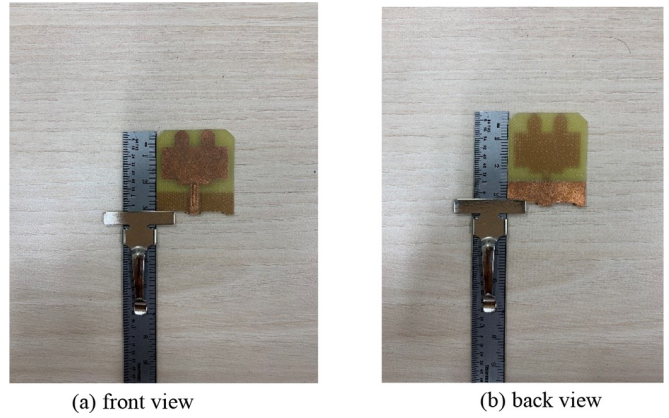
The antenna is simulated using HFSS software that implements Finite Element Method (FEM) and then the fabricated prototype is measured on a one-meter rolled-edge ground plane in an anechoic chamber. The antenna setup inside the chamber is shown in Fig. 3 where an SMA connector is being used to connect the antenna feed point with the chamber's measurement coaxial cable.

Fig. 4 shows a comparison between the simulated and measured VSWR of the proposed design. It can be depicted from the results that the performance of VSWR is better than (2:1) across the whole frequency band (1.71GHz to 5GHz). Fig. 4 also shows good agreement of antenna impedance between simulated model and fabricated prototype with minor differences due to antenna placement on ground plane and small cable loss across frequency bands. In addition, Fig. 4 shows a reasonable rejection for GNSS and DSRC bands which makes the design suitable to be integrated with multiple application in a single housing. Fig. 5 shows the effect on bandwidth impedance of the PGP
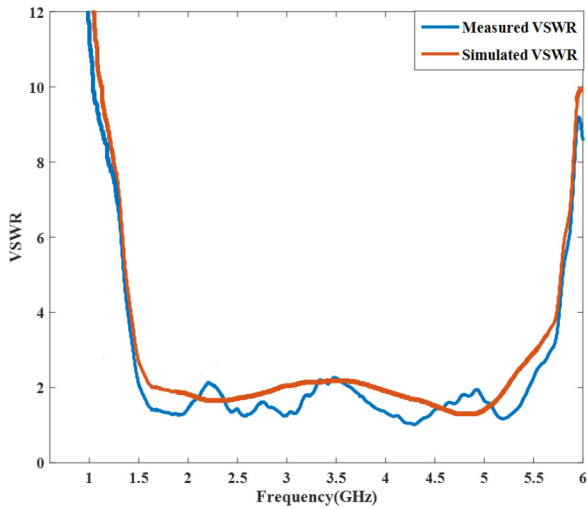
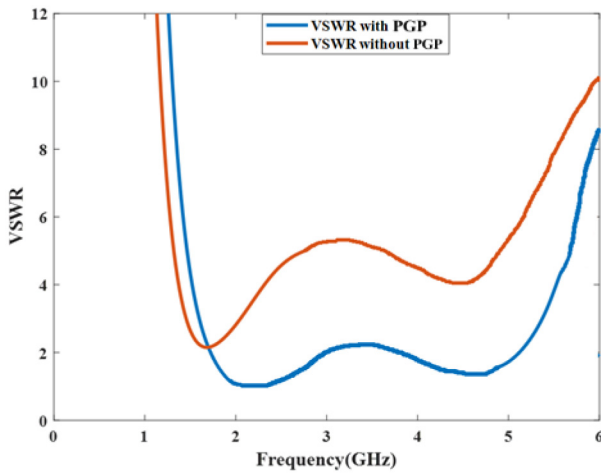**FIGURE 4.** Measured and simulated VSWR on ground plane.

FIGURE 5. Comparison of simulated VSWR with and without partial ground plane structure on the back side of the element.

shape that is placed on the back side of the element. The VSWR gets better with around 2.5 across the entire 5G band when the rectangular ground plane is implemented which is essential to meet the impedance matching requirement for the design.

The surface current distribution and electric field intensity on the front and back side of the element is shown in Fig. 6. The magnitudes are shown in decibels (dB) which is acquired by obtaining the magnitude of magnetic field (H-field) measured in (A/m) and electric field (E-field) measured in (V/m) then applying the formulas:

$$\text{Surface Current (dB)} = 20 * \log(|H(A/m)|) \qquad (1)$$

$$\text{E-field (dB)} = 20 * \log(|E(V/m)|) \qquad (2)$$

It can be concluded that at low frequencies, the current distribution is more intense and spread across the entire structure of the antenna up to the two branches. However, when increasing the frequency band, the current supports shorter paths to radiate at higher frequencies.
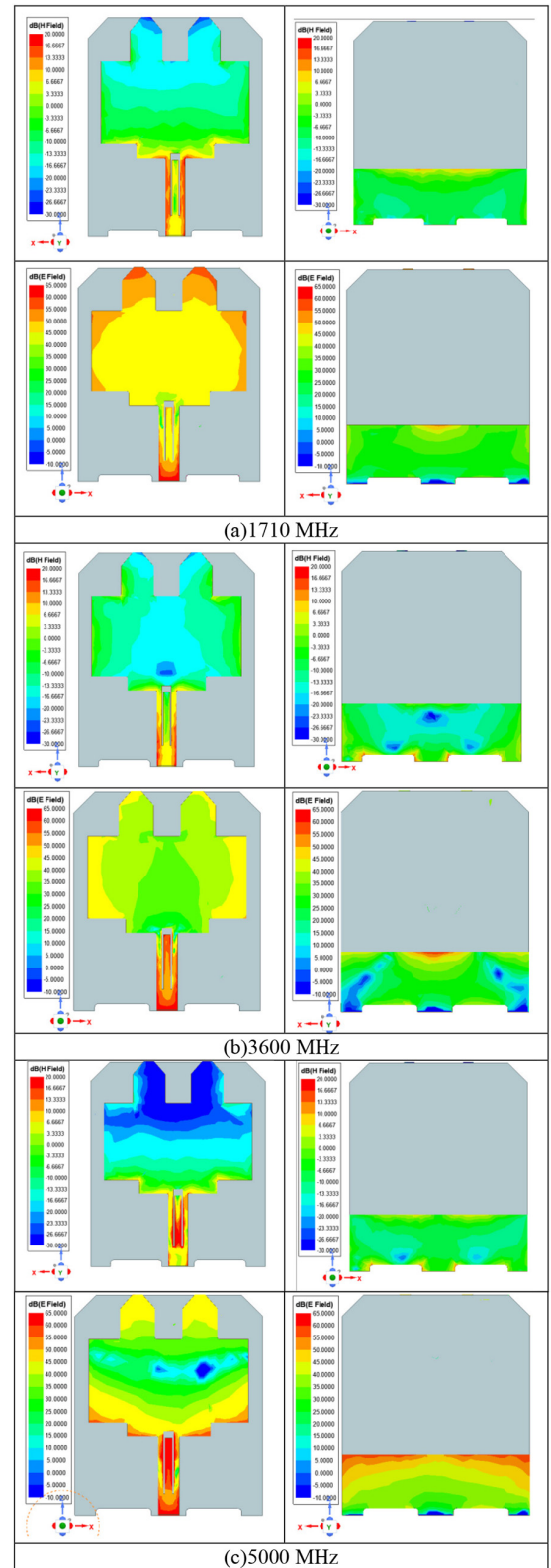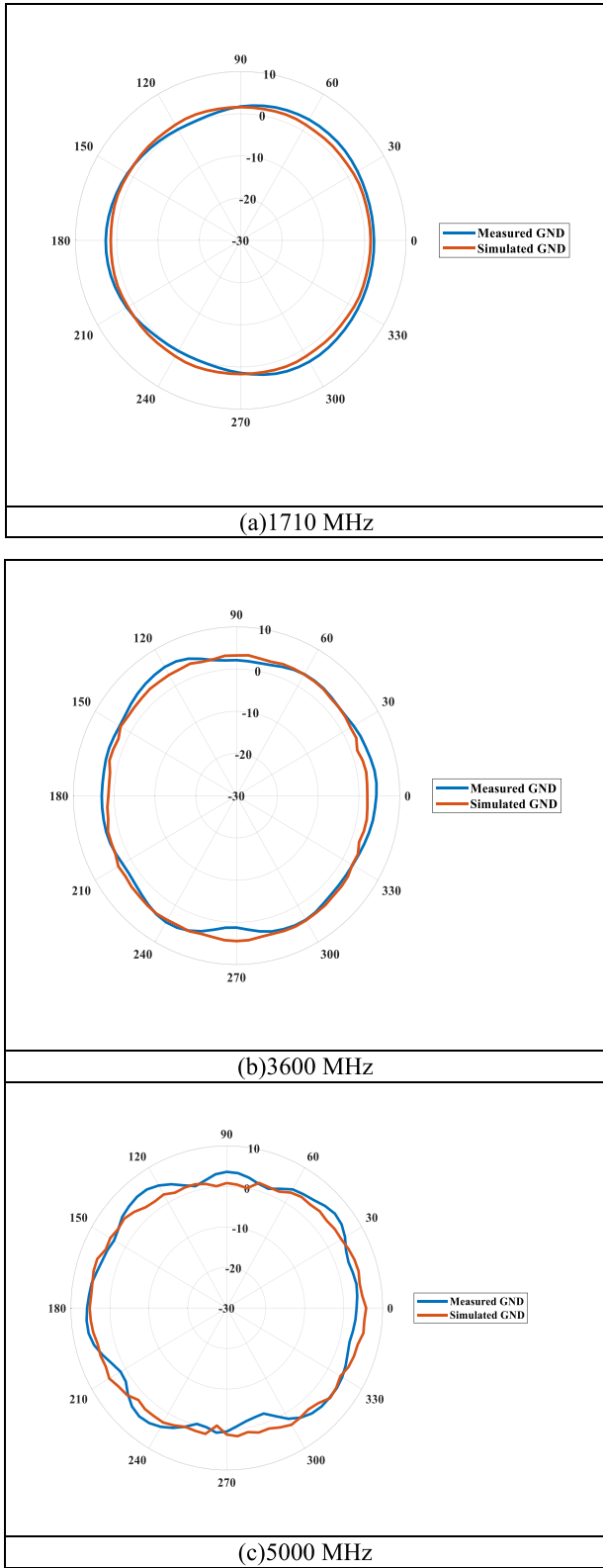

FIGURE 6. Current distribution and electric field intensity measured in (dB) on the front and back side of the antenna: (a) 1710MHz, (b) 3600MHz, and (c) 5000MHz.

The effect of PGP on the current is also shown in Fig. 6 across different frequencies. It can be concluded that a significant amount of in-phase current is going

(a)1710 MHz

(b)3600 MHz

(c)5000 MHz

FIGURE 7. Horizontal cuts of radiation patterns of simulated and measured on GND gain in (dBi) at theta equals 80 degrees: (a) 1.71GHz, (b) 3.6GHz, and (c) 5GHz.

through the partial ground plane shape which helps improving the impedance bandwidth across the whole band.
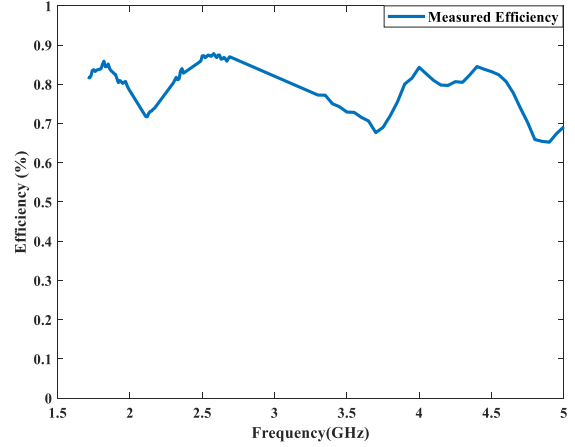
FIGURE 8. Measured antenna radiation efficiency on ground plane.

For optimal performance of 5G antenna on vehicle, it is important to have an omni directional radiation pattern for theta between 75-87 degrees across the operating frequency bands. In Fig. 7, horizontal cuts of the radiation patterns with vertical polarization at theta equals 80 degrees are plotted at multiple frequencies (1.71GHz, 3.6GHz, and 5GHz). The data traces present a comparison of radiation patterns of the simulated model on 1-meter ground plane against fabricated prototype radiation measurements on one-meter rolled-edge ground plane. It can be noticed from Fig. 7 plots that both simulation and measurement have a very good omni directional behavior across the whole operating bands, even though at high frequencies, the pattern shapes get a bit squinted at the sides (azimuth angles 90 and 270 degrees) but still have a very good omni directional shape across the entire azimuth angles with lowest gain value around 0dBi. Furthermore, the average gain obtained from ground plane measurements inside the chamber is found to be 1.75dBi, 3.20dBi, and 3.32dBi at frequencies 1.71GHz, 3.6GHz, and 5GHz, respectively, which indicates an excellent radiation performance of this antenna at 5G bands.

The measured antenna radiation efficiency is shown in Fig. 8. It is obtained as a ratio of the power radiated from the antenna to the power delivered to the antenna's input. In another words, it describes how much of the delivered input power is being radiated by the antenna. It can be noticed from Fig. 8 that the minimum radiation efficiency is about 65% with total average efficiency of 74.4% which shows a very good radiation properties of the proposed design that makes very suitable for 5G application in automotive industry.

The measured LAG of the antenna (in dBi) is shown in Fig. 9. LAG is computed by calculating the average summation across the azimuth (phi) of linear average gain at every theta angle from 75 to 87 degrees across the whole frequency band than converting the results to dBi by using the formula:

$$\text{LAG (dBi, f)} = 10 * \log(\text{average gain across phi}) \quad (3)$$
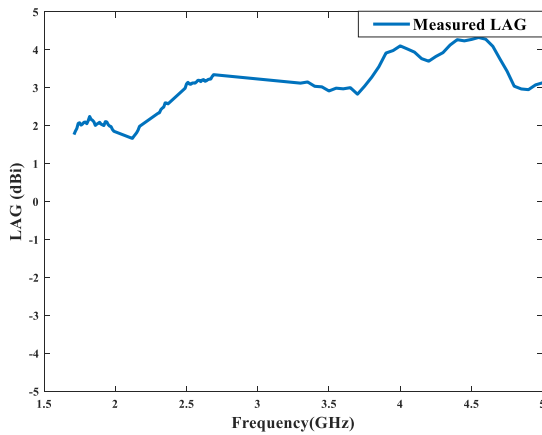
FIGURE 9. Measured LAG in dBi on ground plane across 5G band.

Fig. 9 shows that minimum value of LAG is found to be 1.7dBi with most of operating frequency range having better than 3dBi which gives an excellent gain performance for the proposed antenna.

III. PROPOSED 2X2 MIMO ANTENNA SYSTEM

In this section, two identical elements of the proposed antenna in the previous section are placed on the same Printed Circuit Board (PCB) with a spatial distance of 80mm (approximately 0.5 lambda of the smallest frequency in the band "1.71GHz"). Each antenna element is orientated on the opposite direction of each other (mirrored across z-axis) as shown in Fig. 10 where the simulation and ground plane measurement setups for the proposed MIMO system is presented. The defected ground plane structure of each element is facing each other which is optimal for isolation improvement.

Fig. 11 presents the passive isolation between the two antennas. Both measured and simulated isolation are in good agreement across the whole frequency band with minor differences due to antennas placement on PCB and small attenuation from RF cables at different frequencies. It can be noticed that the worst mutual coupling between the two antennas has passive isolation of 16 dB at the lower bands of the operating frequencies since the RF wavelengths are longer at these frequencies. However, most of the frequency points have better isolation than 20dB as shown in Fig. 11 which shows a good isolation in the system. Fig. 12 shows the difference in passive isolation on simulation model with and without PGP shape on the back side of the element. The existence of the rectangular ground plane improves the isolation by approximately 3dB across the whole frequency bands.

In Fig. 13, horizontal cuts of combined radiation patterns at theta 80 degrees are plotted for multiple frequencies 1.71GHz, 3.6 GHz, and 5GHz. The radiation patterns are measured by measuring one antenna while terminating the other antenna with 50 ohms then the two measurements are combined to get the total radiation pattern of the MIMO
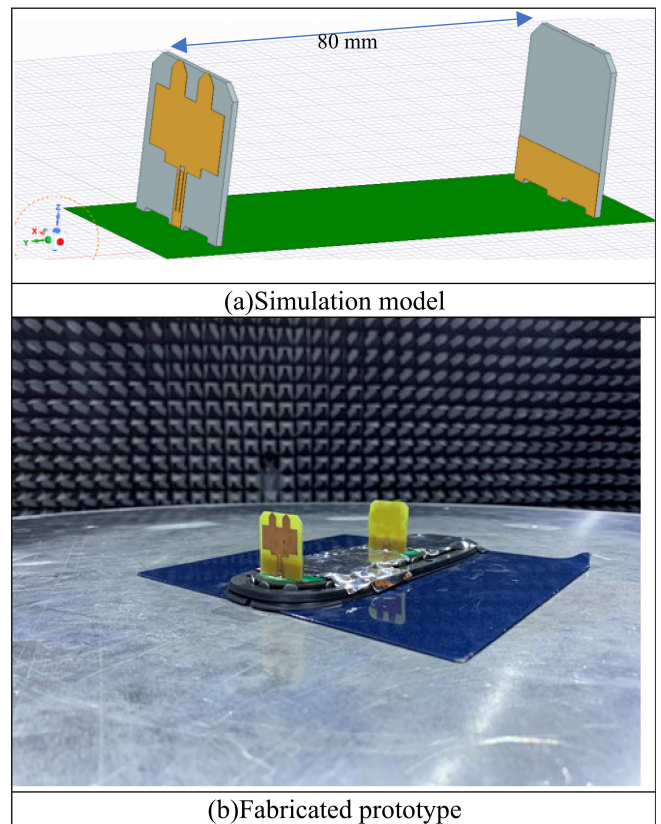

(a)Simulation model

(b)Fabricated prototype

FIGURE 10. Simulation model and prototype measurement setup for proposed MIMO system: (a) Simulation model. (b) Fabricated prototype.
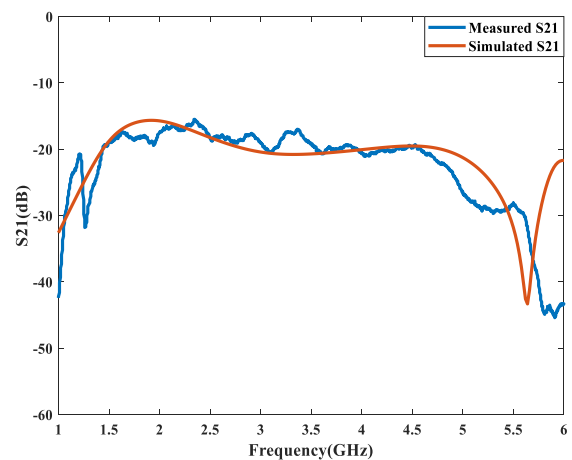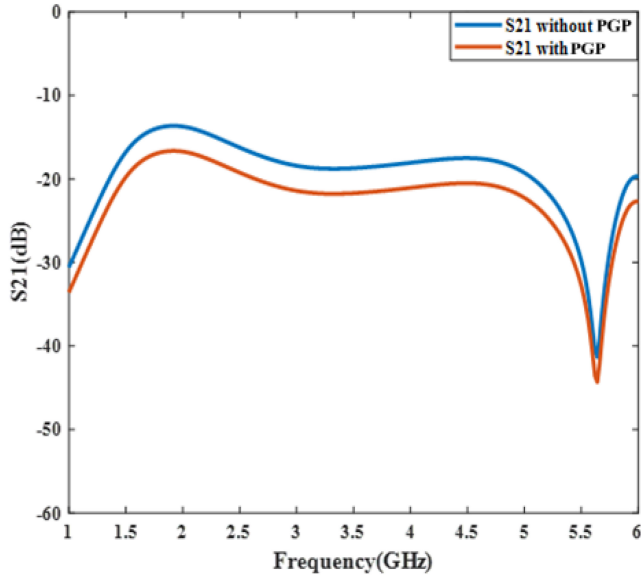

FIGURE 11. Passive isolation measured in dB of simulation model and prototype.

system. Fig. 13 also shows a very good omni directional behavior across the bands which is significant requirement for the RF coverage around the MIMO system. Moreover, the combined average gain observed from the measured radiation patterns is found to be 3.15dBi, 5.12dBi, and 5.22dBi at frequency points 1.71GHz, 3.6GHz, and 5GHz, respectively.

The ECC and DG of the proposed MIMO system is presented in Fig. 14. and Fig. 15. The ECC has

FIGURE 12. Passive isolation measured in dB with and without defected ground plane structure.

been calculated using the electric field components formula [7], [9], [10]:

$$\rho_{e,ij} = \left| \frac{\int_0^{2\pi} \int_0^{\pi} (XPR \cdot E_{\theta i} \cdot E_{\theta j}^* \cdot P_\theta + XPR \cdot E_{\phi i} \cdot E_{\phi j}^* \cdot P_\phi)\sin(\theta)d\theta d\phi}{\sqrt{\prod_{k=i,j} \int_0^{2\pi} \int_0^{\pi} \left(XPR \cdot E_{\theta k} \cdot E_{\theta k}^* \cdot P_\theta + XPR \cdot E_{\varphi k} \cdot E_{\varphi k}^* \cdot P_\phi\right)\sin(\theta)d\theta d\phi}} \right|^2 \quad (4)$$

where $E_{\theta i}$ and $E_{\theta j}$ represent the E-field complex components in the theta direction for the first and second elements (i, and j). $E_{\varphi i}$ and $E_{\varphi j}$ are also the complex E-field components but in the phi direction. XPR is the cross-polarization factor that takes into account the difference in wave polarization (vertical or horizontal) of the received wave. P_θ and P_φ represent the power densities for theta and phi angles. To simply the calculations for equation (4), uniform power densities can be assumed across elevation and azimuth angles, and XPR could be equal to 1 to assume no polarization differences between the antennas.

The diversity gain which is known to be as the quantified improvent in signal-to-noise ratio when the antennas in the MIMO system receives the RF signal and is calculated by the formula [16]:

$$DG = 10 * \sqrt{(1 - \rho)} \quad (5)$$

The electric field components were extracted from the ground plane measurements which include the amplitude and phase of E-field in theta and phi planes then a MATLAB script process the electric field data using the above equations. It can be shown from Fig. 14 that the worst-case of ECC value is about 0.05 that corresponds to DG of 9.98dB which shows the antennas are highly uncorrelated across the 5G bands which is crucial requirement for the MIMO performance.

(a)1710 MHz

(b) 3600 MHz

(c) 5000 MHz
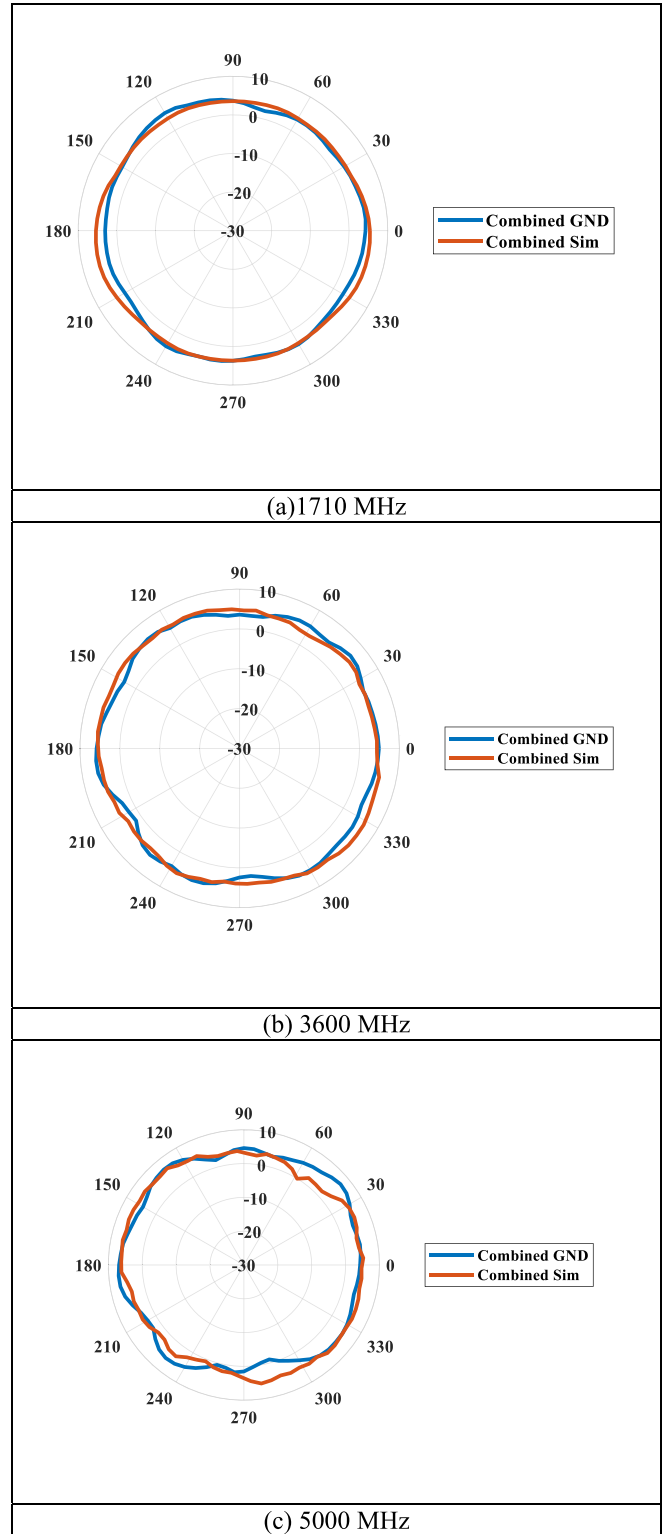
FIGURE 13. Comparison of combined radiation patterns of simulation and ground plane measurements in (dBi) at theta equals 80 degrees: (a) 1.71GHz, (b) 3.6GHz, and (c) 5GHz.

A comparison between proposed design in this paper and existing work in literature is presented in Table3. The proposed design operates on wide frequency range on 5G
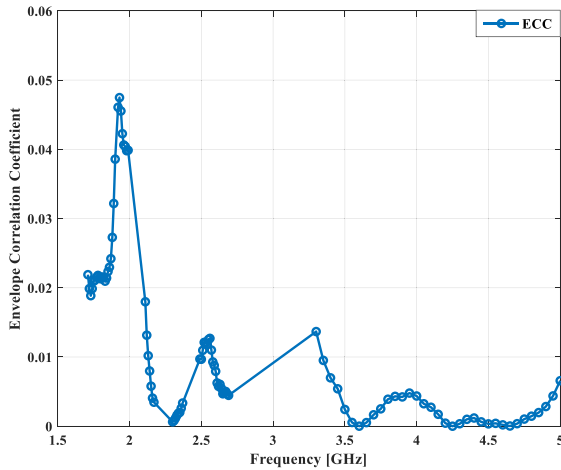
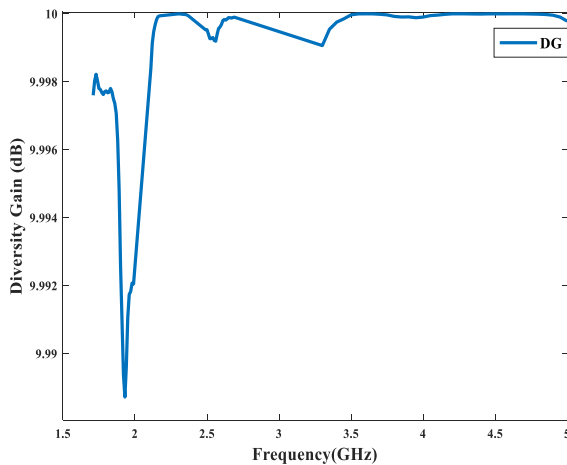**FIGURE 14.** ECC values for ground plane measurements.

FIGURE 15. Diversity gain in dB for ground plane measurements.

bands with very good performance in terms of matched impedance, gain, omni directional radiation patterns, and efficiency.

IV. CONCLUSION

A compact raised printed monopole antenna has been analyzed in this paper to be used in automotive applications that operates on the 5G middle and high frequency bands from 1.71GHz to 5GHz. The design consists of a slotted feed line exciting wide rectangular shape with two branches. The slot in the feed line, upper two branches and the dielectric material (FR4) are used to further tune the antenna towards lower frequency bands. PGP structure has been implemented on the back side of the antenna to provide higher isolation and improve bandwidth impedance. Simulation model was built using HFSS software and then a prototype was measured on one-meter rolled-edge ground plane in an anechoic chamber. The performance of the design shows VSWR

TABLE 3. Comparison between presented element and literature.

	Type	Frequency Bandwidth	Dimensions (LxWxH) (mm3)	VSWR/Gain/ Efficiency
Proposed Design	Raised printed monopole	1.71GHz-5GHz	27x1x30	(2:1) VSWR from 1.71GHz-5GHz. Peak gain 3.7dBi @1.71GHz, 5.4dBi @3.6GHz, and 6.7dBi @5GHz. Avg. radiation efficiency 74.4% on GND
12	Patch antenna with slots and stubs	3.7GHz-5.05GHz	30x1.6x30	(2:1) VSWR. Peak gain 5dBi, Avg. gain 1.5dBi @3.6GHz, 2dBi @5GHz
13	Flagged shape printed antenna	3GHz-6GHz	36x1.6x66	(1.5:1) VSWR. Peak gain 3.28dBi @3.1GHz
14	Printed planar monopole	698MHz-2700MHz	52x1.6x65	(2.6:1) VSWR. Max gain 1.68dBi @700MHz, 5.95dBi @1.8GHz, 3,34dBi @2.3GHz, 3.76dBi @2.7GHz
15	Printed monopole	698MHz-2690MHz	25x2x55	(2.5:1) VSWR. Max gain -0.7 to 5dBi
17	printed antenna	3.34GHz-3.87GHz	20x1.6x35	(2:1) VSWR. Peak gain 2.34dBi
18	Printed monopole with two branches	720MHz-960MHz 1.6GHz-4GHz	30x1.6x70	(2:1) VSWR. Max gain 5.89dBi @2.4GHz, 3.52dBi @3.5GHz
19	Printed Yagi-Uda	2.9GHz-4.1GHz	60x1.6x55	(2.1:1) VSWR. Peak gain higher than 7dBi

performance better than 2:1 with average radiation efficiency of 74.4% on ground plane. LAG was measured from theta equals 75 to 87 degrees with minimum value of 1.7dBi while having higher than 3dBi across most frequency points. A 2x2 MIMO system was analyzed and presented using two identical elements of the proposed design but with different orientation. The MIMO system shows a passive isolation better than 16dB, ECC lower than 0.05, and DG higher than 9.98dB across the operating frequency bands. In general, the presented antenna design in this paper is suitable to be used

for 5G vehicular applications inside shark-fin housing due to its reasonable dimensions and good RF performance.

ACKNOWLEDGMENT

REFERENCES

[1] M. O. Khalifa, A. M. Yacoub, and D. N. Aloi, "A multiwideband compact antenna design for vehicular sub-6 GHz 5G wireless systems," *IEEE Trans. Antennas Propag.*, vol. 69, no. 12, pp. 8136–8142, Dec. 2021.

[2] A. Yacoub, M. Khalifa, and D. N. Aloi, "Wide bandwidth low profile PIFA antenna for vehicular sub-6 GHz 5G and V2X wireless systems," *Progr. Electromagn. Res. C*, vol. 109, pp. 257–273, Jan. 2021.

[3] J. Huang, C.-X. Wang, H. Chang, J. Sun, and X. Gao, "Multi-frequency multi-scenario millimeter wave MIMO channel measurements and modeling for B5G wireless communication systems," *IEEE J. Sel. Areas Commun.*, vol. 38, no. 9, pp. 2010–2025, Sep. 2020, doi: 10.1109/JSAC.2020.3000839.

[4] Yacoub, A. and Aloi, D., "Low profile PIFA antenna for vehicular 5G and DSRC communication systems," Soc. Autom. Eng., Warrendale, PA, USA, SAE Tech. Paper 2021–01-0150, 2021.

[5] H. Ullah, N. G. Nair, A. Moore, C. Nugent, P. Muschamp, and M. Cuevas, "5G communication: An overview of vehicle-to-everything, drones, and healthcare use-cases," *IEEE Access*, vol. 7, pp. 37251–37268, 2019.

[6] C.-X. Wang, J. Bian, J. Sun, W. Zhang, and M. Zhang, "A survey of 5G channel measurements and models," *IEEE Commun. Surveys Tuts.*, vol. 20, no. 4, pp. 3142–3168, 4th Quart. 2018.

[7] A. Yacoub, M. Khalifa, and D. N. Aloi, "Compact 2 × 2 automotive MIMO antenna systems for sub-6 GHz 5G and V2X communications," *Progr. Electromagn. Res. B*, vol. 93, 23–46, Jan. 2021.

[8] M. O. Khalifa, A. M. Yacoub, and D. N. Aloi, "Compact 2x2 and 4x4 MIMO antenna systems for 5G automotive applications," *Appl. Comput. Electromagn. Soc.*, vol. 36, no. 6, pp. 762–778, 2021.

[9] A. M. Elshirkasi, A. A. Al-Hadi, M. F. Mansor, R. Khan, and P. J. Soh, "Envelope correlation coefficient of a two-port MIMO terminal antenna under uniform and Gaussian angular power spectrum with user's hand effect," *Progr. Electromagn. Res. C*, vol. 92, pp. 123–136, Apr. 2019.

[10] M. S. Sharawi, A. T. Hassan, and M. U. Khan, "Correlation coefficient calculations for MIMO antenna systems: A comparative study," International Journal of Microwave and Wireless Technologies, vol. 9, no. 10, pp. 1991–2004, 2017.

[11] G. Artner, W. Kotterman, G. D. Galdo, and M. A. Hein, "Automotive antenna roof for cooperative connected driving," *IEEE Access*, vol. 7, pp. 20083–20090, 2019.

[12] J. Karthi, "A novel UWB MIMO antenna with high isolation for sub-6 GHz band application," *Turkish J. Comput. Math. Educ.*, vol. 12, no. 12, pp. 1934–1943, 2021.

[13] N. Supreeyatitikul, A. Phungasem, and P. Aeimopas, "Design of wideband sub-6 GHz 5G MIMO antenna with isolation enhancement using an MTM-inspired resonators," in *Proc. Joint Int. Conf. Digit. Arts Media Technol. ECTI Northern Sec. Conf. Elect. Electron. Comput. Telecommun. Eng.*, 2021, pp. 206–209.

[14] D. Preradovic and D. N. Aloi, "Cross polarized 2x2 LTE MIMO system for automotive shark fin application," *Appl. Comput. Electromagn. Soc.*, vol. 35, no. 10, pp. 1207–1216, Oct. 2020.

[15] Liu, Y., Z. Ai, G. Liu, and Y. Jia, "An integrated shark-fin antenna for MIMO-LTE, FM, and GPS applications," *IEEE Antennas Wireless Propag. Lett.*, vol. 18, no. 8, pp. 1666–1670, Aug. 2019.

[16] S. F. Beegum and S. K. Mishra, "Compact WLAN band-notched printed ultrawideband MIMO antenna with polarization diversity," *Progr. Electromagn. Res. C*, Vol. 61, pp. 149–159, Jan. 2016.

[17] A. K. Saurabh and M. K. Meshram," "Compact sub-6 GHz 5G-multiple-input-multiple-output antenna system with enhanced isolation," *Int. J. RW Microw. Comput. Aided Eng.*, vol. 30, no. 8, Aug. 2020, Art. no. e22246.

[18] Y. Cheng, J. Lu, and C. Wang, "Design of a multiple band vehicle-mounted antenna," *Int. J. Antennas Propag.*, vol. 2019, Dec. 2019, Art. no. 6098014. [Online]. Available: https://doi.org/10.1155/2019/6098014

[19] K. Sreelakshmi, P. Bora, M. Mudaliar, Y. B. Dhanade, and B. T. P. Madhav, "Linear array Yagi-Uda 5G antenna for vehicular application," *Int. J. Eng. Technol.*, vol. 7, pp. 513–517, Jan. 2018.

[20] N. Jaglan, S. D. Gupta, B. K. Kanaujia, and M. S. Sharawi, "10 element sub-6-GHz multi-band double-T based MIMO antenna system for 5G smartphones," *IEEE Access*, vol. 9, pp. 118662–118672, 2021.

[21] N. Jaglan, S. D. Gupta, and M. S. Sharawi, "18 element massive MIMO/diversity 5G smartphones antenna design for sub-6 GHz LTE bands 42/43 applications," *IEEE Open J. Antennas Propag.*, vol. 2, pp. 533–545, 2021.
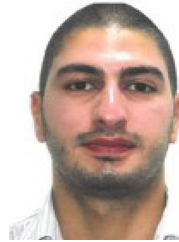
AHMAD M. YACOUB received the B.S. degree in electrical engineering from the Princess Sumaya University for Technology, Amman, Jordan, in 2014, and the M.S. degree in electrical and computer engineering from Oakland University, Rochester, MI, USA, in 2018, where he is currently pursuing the Ph.D. degree in electrical and computer engineering.

He served as a Research Assistant with the Applied EMAG and Wireless Lab, Oakland University from 2016 to 2018. He has been employed with Molex LLC, Grand Blanc, MI, USA, since 2018. He is an inventor/co-inventor of two patents. His research interests reside in area of applied electromagnetics with emphasis on antenna measurements, antenna modeling/analysis, and antenna design.

MOHAMED O. KHALIFA received the B.S. degree in electrical and electronic engineering from the University of Khartoum, Khartoum, Sudan, in 2010, and the M.S. degree in electrical engineering from the King Fahd University of Petroleum and Minerals, Dhahran, Saudi Arabia, in 2015. He is currently pursuing the Ph.D. degree in electrical and computer engineering with Oakland University.

He served as a Research Assistant with the King Fahd University of Petroleum and Minerals, a Visiting Graduate Intern with I-Radio Lab, School of Engineering, University of Calgary in Alberta, Canada, and a Research Assistant with the Applied EMAG and Wireless Lab, Oakland University from 2012 to 2018. He was employed with Ficosa North America, Madison Heights, MI, USA, from 2018 to 2019 and has been with Molex LLC, Grand Blanc, MI, USA, since 2019. He has authored/coauthored around six technical papers and is an inventor on three patents. His research interests reside in area of power amplifier design and linearization techniques and applied electromagnetics with emphasis on antenna measurements, antenna modeling/analysis, and antenna design.

DANIEL N. ALOI (Senior Member, IEEE) received the B.S., M.S., and Ph.D. degrees in electrical engineering from Ohio University, Athens, OH, USA, in 1992, 1996, and 1999, respectively. He served as a Research Assistant with the Avionics Engineering Center, School of Engineering and Computer Science, Ohio University from 1995 to 1999; a Summer Intern with Rockwell International, Cedar Rapids, IA, USA, and a Senior Project Engineer with OnStar, Incorporated, a subsidiary of General Motors from 2000 to 2002.

He has been employed with the Electrical and Computer Engineering Department, Oakland University, Rochester, MI, USA, since 2002, where he is the Founder and the Director of the Applied EMAG and Wireless Lab. He has authored/coauthored over 100 technical papers and is an inventor on five patents. His research interests reside in area of applied electromagnetics with emphasis on antenna measurements, antenna modeling/analysis, and antenna design. He is a member of the Institute of Navigation. He has received in excess of $4M in research funding from a variety of federal and private entities, including the Federal Aviation Administration, Defense Advanced Research Program Agency, and the National Science Foundation.